Statistical Mechanical Understanding of Two-Dimensional Point Vortex System at Negative Absolute Temperature

Yuichi YATSUYANAGI

Faculty of Education, Shizuoka University, Shizuoka 422-8529, Japan

(Received: 1 September 2008 / Accepted: 16 November 2008)

Statistical characteristics of two-dimensional point vortex systems in positive and negative temperature states are examined by massive numerical simulations using a special-purpose supercomputer, MDGRAPE-3. Mathematical description of the system is identical to that of a collection of charged rods, i.e., a guiding-center plasma. The characteristics of the negative temperature state is examined by a numerically obtained density of state, time-asymptotic equilibrium distributions and energy spectra at various values of temperature. The density of state has a peak and it is confirmed that the target point vortex system has the negative temperature state. In the negative temperature case, the equilibrium distribution has a dipolar structure while in the positive temperature case, the vortices spread uniformly inside the circular boundary. Slope of the energy ($k-$) spectrum in the intermediate k region becomes steep as energy increases.

Keywords: negative temperature state, point vortex system, guiding-center plasma, k-spectrum, MDGRAPE-3

1. Introduction

Large-scale, long-lived vortices are commonly observed in nearly two-dimensional flow. Onsager introduced a concept of "negative temperature" for the two-dimensional point vortex system in 1949 to understand the large-scale vortex formation [1]. The temperature T is statistically defined by

$$\frac{1}{T} = \frac{\partial S}{\partial E} = k_B \frac{\partial \ln W(E)}{\partial E}. \tag{1}$$

In usual cases, the density of state $W(E)$ increases as energy E increases, and the slope $\partial S/\partial E$ never changes the sign and is always positive. On the other hand, if the total phase space volume is finite, the total number of states is limited, and the asymptotic value of the density of state at infinite energy must be zero. Then the density of state should have at least a peak at some energy E_0 and the temperature is negative at $E > E_0$. Onsager considered the phase space is identical to the configuration space in the two-dimensional point vortex system. If the vortices are confined in a finite area, total configuration space, i.e., total phase space is also finite. Thus, Onsager concluded that the negative temperature state appears in the two-dimensional point vortex system confined in a finite area.

It must be emphasized that the temperature in the Onsager theory is defined not in the (thermo-) dynamical sense, but in the statistical sense. There is no negative temperature state in the dynamical sense, although the temperatures defined statistically and dynamically coincide with each other in positive temperature. So we have set up a target of this research to understand the characteristics of the negative temperature appearing in the two-dimensional point vortex system in the dynamical sense.

In this paper, we present our simulation results. In §2, a target point vortex system is introduced. In §3, we briefly explain a simulation system. In §4, simulation results of a density of state, equilibrium distributions and energy spectra are given. In §5, we summarize our results.

author's e-mail: eyyatsu@ipc.shizuoka.ac.jp

2. Point vortex system

Let us consider a point vortex system consisting of $N/2$ positive and $N/2$ negative point vortices with circulation Γ_0 (= Constant) and $-\Gamma_0$, respectively, bounded by a circular wall with radius R [2]. Typical value of the total number of vortices N is 6724. The position vector and the circulation of the i-th point vortex are given by $\boldsymbol{r}_i$ and Γ_i, respectively. Constants of motion are Hamiltonian and inertia:

$$\begin{aligned} H &= -\frac{1}{4\pi}\sum_{i}^{N}\sum_{j\neq i}^{N}\Gamma_i\Gamma_j \ln|\boldsymbol{r}_i - \boldsymbol{r}_j| \\ &\quad +\frac{1}{4\pi}\sum_{i}^{N}\sum_{j}^{N}\Gamma_i\Gamma_j \ln|\boldsymbol{r}_i - \bar{\boldsymbol{r}}_j| \\ &\quad -\frac{1}{4\pi}\sum_{i}^{N}\sum_{j}^{N}\Gamma_i\Gamma_j \ln\frac{R}{|\boldsymbol{r}_j|}, \end{aligned} \tag{2}$$

$$I = \sum_{i}^{N}\Gamma_i|\boldsymbol{r}_i|^2 \tag{3}$$

The wall effect is introduced by the image vortices located at $\bar{\boldsymbol{r}}_i = R^2\boldsymbol{r}_i/|\boldsymbol{r}_i|^2$. The last term in Eq. (2) is introduced to make the value of stream function at the circular wall zero. Equations of motion for each point vortex are given by

$$\Gamma_i\frac{dx_i}{dt} = \frac{\partial H}{\partial y_i}, \quad \Gamma_i\frac{dy_i}{dt} = -\frac{\partial H}{\partial x_i}, \tag{4}$$

or explicitly

$$\begin{aligned} \frac{d\boldsymbol{r}_i}{dt} &= -\frac{1}{2\pi}\sum_{j\neq i}^{2N}\Gamma_j\frac{(\boldsymbol{r}_i - \boldsymbol{r}_j)\times\hat{\boldsymbol{z}}}{|\boldsymbol{r}_i - \boldsymbol{r}_j|^2} \\ &\quad +\frac{1}{2\pi}\sum_{j}^{2N}\Gamma_j\frac{(\boldsymbol{r}_i - \bar{\boldsymbol{r}}_j)\times\hat{\boldsymbol{z}}}{|\boldsymbol{r}_i - \bar{\boldsymbol{r}}_j|^2}. \end{aligned} \tag{5}$$

Right hand side of Eq. (5) is the Biot-Savart integrals.

3. MDGRAPE-3

A difficulty in the point vortex simulations comes from a calculation cost of the Biot-Savart integral proportional to O(N^2). In addition, the cost is twice as large as the one with no boundary, if the boundary effect is introduced by the image vortices. There are some solutions for this problem, for example, using a fast algorithm, using a fast computer and so on. We have selected a way to use a fast computer.

Fig. 1 MDGRAPE-3 is a PCI-X add-on card that needs to be installed on a PC.

In general, to speed up calculations in a central processing unit (CPU), it is very efficient to restrict the types of calculation, i.e., reducing the instruction set, and to implement the instructions as a wired-logic device completely [3]. An extreme example is a special-purpose computer that can calculate usually only one kind of calculation. We have used the special-purpose computer called MDGRAPE-3 shown in Fig. 1 [4]. It was originally developed for acceleration of forces with O(N^2) calculation cost needed for molecular dynamics simulations, e.g., Coulomb force and Van der Waals force. Furthermore, it has an ability to accelerate calculations of forces expressed as a function of distances between particles in a system $|\boldsymbol{r}_i - \boldsymbol{r}_j|^2$. As we have noticed that the Biot-Savart integral in the two-dimensional point-vortex system meets the above conditions, we have used MDGRAPE-3 to accelerate the two-dimensional point-vortex simulations. For $N = 8036$ vortex case, a calculation time of one time step is 6.01 second by a normal PC and 0.068 second by MDGRAPE-3. Namely, MDGRAPE-3 finishes a simulation within a day, while it takes 89 days with a normal PC.

4. Simulation results

In this section, we demonstrate the simulation results for the statistical understanding of the two-dimensional point vortex system [5].

4.1 Density of state

To confirm an existence of the negative temperature state in the target point vortex system, a density of state is obtained by a random sampling of states following the micro canonical statistics. Each state is classified by the energy E and the inertia I which are determined by randomly generated distribution of the point vortices. Density of state consisting of 10^8 states is shown in Fig. 2.

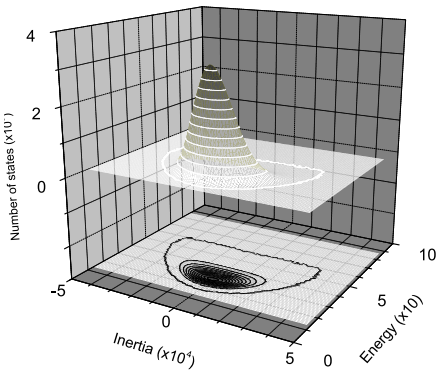

Fig. 2 Density of state is plotted against system energy E and inertia I. The peak is located at $E_0 = 29.1$ and $I_0 = 0.0$.

The density of state has a peak at $E = 29.1(\equiv E_0)$ and $I = 0.0(\equiv I_0)$, which gives an evidence for the existence of the negative temperature state. Namely, the temperature is negative at $E > E_0$. The ridge extends on $I = 0$ plane that is a symmetric plane of the density of state. As the number of vortices increases, the peak becomes steep one and peak position approaches $E = 0$.

4.2 Equilibrium distributions

Equilibrium distributions of the vortices at various values of temperature are obtained time-asymptotically by time development simulations. The temperature is controlled by the initial distribution of the vortices that determines the system energy. The results are shown in Fig. 3.

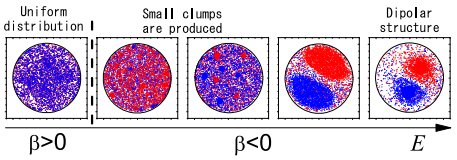

Fig. 3 Equilibrium distributions of the vortices are shown. The leftmost distribution corresponds to the positive temperature case. As the system energy increases, small clumps are gradually produced and finally reaches a dipolar configuration as is seen in the rightmost distribution. In the rightmost distribution, the upper and lower clumps exclusively consist of the positive and the negative vortices, respectively.

In positive temperature, both-sign vortices mix with each other and spread over the circular area uniformly. On the other hand, when the sign of the temperature changes with energy increase, the same-sign vortices tend to form small clumps. As the energy increases further, each clump size becomes gradually large and the configuration finally reaches a dipole one. This statistical tendency of the same

sign clustering in the negative temperature region is clear from a description by a canonical energy distribution proportional to $\exp(-\beta E)$ where β is the inverse temperature. Negative β corresponds to reversing the sign of the interaction, where the same-sign vortices statistically attract and opposite ones repel [6].

It must be emphasized that the background vortices enable the clump formation in the energy conserving system. To conserve the total system energy constant, the low-energy background vortices play very important role. Some vortices release their energy and the others gain the energy and form the clumps. The energy belonging to the background vortices is relatively low compared with the vortices in the clumps. This indicates the common and essential role of background vortices in supporting the condensation of two-sign vortices as well as in assisting the generation of symmetric configuration of the non-neutral plasma clumps [7–11].

4.3 Energy spectrum

Energy spectrum of the point vortex system bounded by a circular wall is obtained analytically by [11, 12],

$$
\begin{aligned}
E(k) &= \frac{1}{4\pi k}\sum_{i}^{N}\Gamma_i^2 \\
&\quad + \frac{1}{4\pi k}\sum_{i}^{N}\sum_{j\neq i}^{N}\Gamma_i\Gamma_j J_0\left(k|\boldsymbol{r}_i-\boldsymbol{r}_j|\right) \\
&\quad - \frac{1}{2\pi k}\sum_{i}^{N}\sum_{j}^{N}\Gamma_i\Gamma_j\sum_{\ell=0}^{\infty}\epsilon_\ell\left(\frac{|\boldsymbol{r}_j|}{R}\right)^\ell \\
&\qquad \times J_\ell(kR)J_\ell(k|\boldsymbol{r}_i|)\cos\left(\ell(\varphi_i-\varphi_j)\right) \\
&\quad + \frac{1}{2\pi k}\sum_{i}^{N}\sum_{j}^{N}\Gamma_i\Gamma_j\sum_{\ell=0}^{\infty}\epsilon_\ell\left(\frac{|\boldsymbol{r}_j|}{R}\right)^\ell \\
&\qquad \times J_\ell^2(kR)\cos\left(\ell(\varphi_i-\varphi_j)\right) \qquad (6)
\end{aligned}
$$

$$
\epsilon_\ell = \begin{cases} 1 & \ell = 0, \\ 2 & \ell \geq 1, \end{cases} \qquad (7)
$$

$$
x_i = |\boldsymbol{r}_i|\cos(\varphi_i), \quad y_i = |\boldsymbol{r}_i|\sin(\varphi_i). \qquad (8)
$$

where $J_\ell(x)$ is the ℓ-th Bessel function of the first kind. The first and the second terms in Eq. (6) obtained by Novikov give the spectrum for an unbounded point vortex system, and the rest represents the effect of the circular boundary. We have obtained spectra by using the formula (6) for the time-asymptotic equilibrium distributions at various temperatures. The results for 4 different temperatures (two positive and two negative) are shown in Fig. 4.

Spectrum range is limited by the radius of the boundary in the small k region and by the minimum distance between the vortices in the large k region. As is readily seen, the slope of the intermediate k (from the diameter scale to the minimum distance scale between the vortices) decreases as the energy increases. In Fig. 5, the slope of the intermediate k is plotted against the system energy.

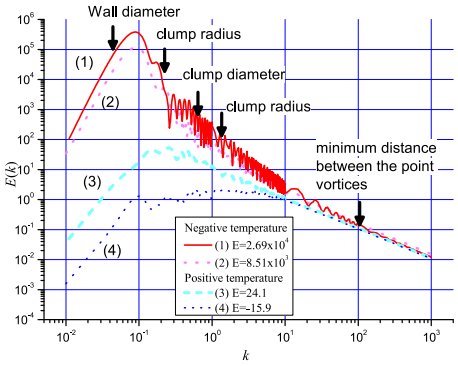

Fig. 4 Energy spectra are plotted at 4 different temperatures. The temperature is controlled by the initial configuration of the vortices. Upper two lines correspond to the negative temperature (high-energy) case and lower two lines correspond to the positive temperature case.

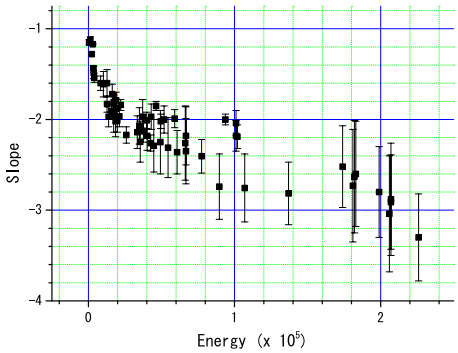

Fig. 5 The slope in the intermediate k is plotted against the system energy.

It can be seen that the negative slope gradually decreases as the energy increases. There are many data around slope= -3. It seems that the asymptotic value of the slope is -3. However, as energy increases, the slope decreases beyond -3. This observation indicates the slope in the intermediate k changes with system energy and is not universal.

In the positive temperature case, the slope should be -1 as the second, third and fourth terms in Eq. (6) cancel each other due to the uniform distribution of the positive and negative vortices, and only the first term remains. However, there is a case where the slope is not -1 as shown in the lowest line in Fig. 4. The difference can be elucidated by a two-body correlation function. The two-body correlation function is defined by a distribution of the distances for all combinations and is normalized by the total number of the combinations of two vortices. The correlation functions are shown in Fig. 6.

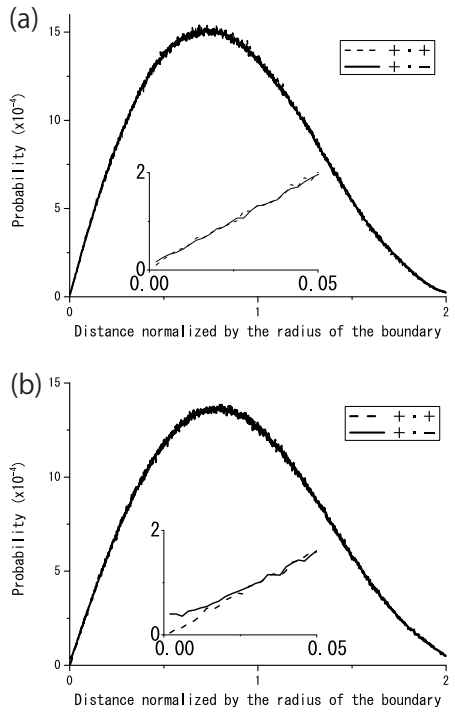

Fig. 6 Two-body correlation functions where (a) the slope of the spectrum is equal to -1 and (b) the slope is unequal to -1 are plotted. In the inset the region of the distances between 0.0 and 0.05 is magnified. It is clearly observed that "+·+" and "+·−" lines do not line up with each other in (b) while do in (a).

The difference appears in the distribution probability of negative vortices around positive vortices indicated by "+ · −" in the plot. In Fig. 6 (a) which corresponds to the slope $= -1$ case, the probability of "+ · −" drops to zero in the limit of zero distance. On the other hand, in Fig. 6 (b) which corresponds to the slope $\neq -1$ case, the value does not drop to zero in the limit of zero distance. As the distribution probability of the positive vortices around the positive vortices and that of the negative vortices around the positive vortices does not match, and the cancellation of the terms in Eq. (6) is imperfect, the slope is not -1. This result suggests that there are at least two equilibrium states as shown in Fig. 7.

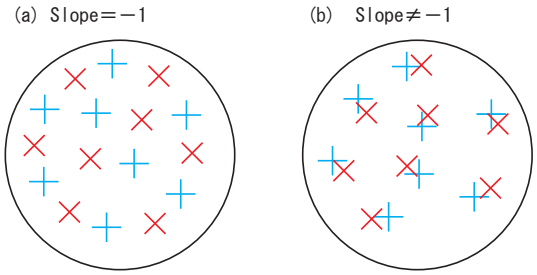

Fig. 7 Two equilibrium distributions are illustrated. The signs + and × represent the positive and negative vortices, respectively.

5. Discussion

In this paper, statistical characteristics of the two-dimensional point vortex systems in positive and negative temperature states has been presented.

On-hand supercomputer, MDGRAPE-3, enables the massive point vortex simulation. The existence of the negative temperature state in the target point vortex system is confirmed by the numerically obtained density of state that has a peak at $E_0 = 29.1$ and $I_0 = 0.0$. In the negative temperature, the same-sign vortices cumulate and form clumps. There is the highest energy configuration where all the positive vortices condense at a point and all the negative vortices condense at the other point. There is no state available larger than the highest energy. In the positive temperature both sign vortices mix with each other and spread out the circular wall. It is revealed by the two-body correlation function that there are at least two different equilibrium configurations in the positive temperature. The configuration corresponding to the slope $= -1$ case appears when temperature is high. On the other hand, the configuration corresponding to the slope $\neq -1$ case appears near zero absolute temperature. So, we can call the latter case "frozen configuration". The slope of the spectrum in the intermediate k region depends on the system energy. As energy increases, the negative slope becomes steep. It may be likely that there is no universal value of the slope.

Acknowledgement

The author thanks Professor Yasuhito Kiwamoto, Professor Hiroyuki Tomita, Dr. Mitsusada M. Sano and Mr. T. Yoshida for valuable discussion. The author thanks Dr. Toshikazu Ebisuzaki, Dr. Makoto Taiji and Dr. Tetsu Narumi for a support of MDGRAPE-2 and MDGRAPE-3. This work was supported by KAKENHI (20740222).

[1] L. Onsager, Nuovo Cimento Suppl., **6**,279 (1949).

[2] P. K. Newton, *The N-Vortex Problem* (Springer-Verlag, Berlin, 2001) chapter 3.
[3] D. Patterson and J. Hennessy, *Computer Organization and Design, 3rd ed.* (Morgan Kaufmann, San Fransisco, 2004).
[4] R. Susukita, T. Ebisuzaki, B. G. Elmegreen, H. Furusawa, K. Kato, A. Kawai, Y. Kobayashi, T. Koishi, G. D. McNiven, T. Narumi, and K. Yasuoka, Comput. Phys. Comm., **155**, 115 (2003).
[5] Y. Yatsuyanagi, Y. Kiwamoto, H. Tomita, M. M. Sano, T. Yoshida, and T. Ebisuzaki, Phys. Rev. Lett., **94**, 054502 (2005).
[6] G. L. Eyink and K. R. Sreenivasan, Rev. Mod. Phys., **78**, 87 (2006).
[7] A. Sanpei, Y. Kiwamoto, K. Ito, and Y. Soga, Phys. Rev. E, **68**, 016404 (2003).
[8] Y. Soga, Y. Kiwamoto, A. Sanpei, and J. Aoki, Phys. Plasmas, **10**, 3922 (2003).
[9] D. Z. Jin and D. H. E. Dubin, Phys. Rev. Lett., **80**, 4434 (1998).
[10] K. S. Fine, A. C. Cass, W. G. Flynn, and C. F. Driscoll, Phys. Rev. Lett., **75**, 3277 (1995).
[11] T. Yoshida and M. M. Sano, J. Phys. Soc. Jpn., **74**, 587 (2005).
[12] E. A. Novikov, Sov. Phys. JETP, **41**, 937 (1975).